

PAPER

2-Step QRM-MLBD for Broadband Single-Carrier Transmission

Katsuhiro TEMMA^{†a)}, Tetsuya YAMAMOTO[†], *Student Members*, Kyesan LEE^{††}, *Member*,
and Fumiyuki ADACHI[†], *Fellow*

SUMMARY Maximum likelihood block signal detection employing QR decomposition and M-algorithm (QRM-MLBD) can significantly improve the bit error rate (BER) performance of single-carrier (SC) transmission while significantly reducing the computational complexity compared to maximum likelihood detection (MLD). However, its computational complexity is still high. In this paper, we propose the computationally efficient 2-step QRM-MLBD. Compared to conventional QRM-MLBD, the number of symbol candidates can be reduced by using preliminary decision made by minimum mean square error based frequency-domain equalization (MMSE-FDE). The BER performance achievable by 2-step QRM-MLBD is evaluated by computer simulation. It is shown that it can significantly reduce the computational complexity while achieving almost the same BER performance as the conventional QRM-MLBD.

key words: single-carrier, QR decomposition, M-algorithm, MMSE-FDE

1. Introduction

The broadband wireless channel is composed of many propagation paths with different time delays and so is characterized as a frequency-selective fading channel. In the frequency-selective fading channel, the bit error rate (BER) performance of single-carrier (SC) transmission severely degrades due to strong inter-symbol interference (ISI) [1]. Although the minimum mean square error based frequency-domain equalization (MMSE-FDE) can significantly improve the BER performance [2], [3], a big performance gap from the matched filter (MF) bound still exists due to presence of the residual ISI after FDE [4].

Maximum likelihood detection (MLD) is the optimum detection for an uncoded additive white Gaussian noise (AWGN) channel with different symbols being transmitted with equal probability [5]. However, MLD has prohibitively high computational complexity. Recently, a maximum likelihood block signal detection employing QR decomposition and M-algorithm (QRM-MLBD) [6] was proposed for the reception of the SC signals transmitted over a frequency-selective fading channel [7], [8]. QRM-MLBD can achieve a BER performance close to the MF bound by increasing the number M of surviving paths in the M-

algorithm [7], [8], while requiring quite reduced complexity compared to MLD. However, its computational complexity is still high compared to MMSE-FDE. To reduce the computational complexity of QRM-MLBD, several methods to reduce the required value of M were proposed [9]–[11]. In addition, the methods to reduce the number of symbol candidate to be involved in the path metric computation were proposed [12]–[16] by performing preliminary decision successively in M-algorithm.

In this paper, we propose another method to reduce the number of symbol candidate to be involved in the path metric computation of QRM-MLBD in which the preliminary decision is made over an entire block using MMSE-FDE prior to conducting the M-algorithm to remove the symbol candidates having low reliability. We call this proposal 2-step QRM-MLBD. In the conventional QRM-MLBD, the path metric is calculated for all symbol candidates at each stage. 2-step QRM-MLBD computes the path metrics only for the limited symbol candidates, and therefore, 2-step QRM-MLBD can further reduce the computational complexity compared to the conventional QRM-MLBD. We evaluate, by computer simulation, the average BER performance of SC transmissions achievable with 2-step QRM-MLBD and compare it to conventional QRM-MLBD.

The remainder of this paper is organized as follows. Section 2 presents the SC transmission with 2-step QRM-MLBD. In Sect. 3, we evaluate the BER performance achievable with our proposed 2-step QRM-MLBD by computer simulation and discuss how much we can reduce the number of symbol candidates. Section 4 offers the conclusion.

2. 2-Step QRM-MLBD

2.1 System Model for SC Signal Transmission

The SC transmission system model with 2-step QRM-MLBD is illustrated in Fig. 1. Throughout the paper, the symbol-spaced discrete time representation is used. At the transmitter, a binary information sequence is data-modulated and then the data-modulated symbol sequence is divided into a sequence of blocks of N_c symbols each, where N_c is the size of discrete Fourier transform (DFT). The data symbol block is expressed using the vector form as $\mathbf{d} = [d(0), \dots, d(N_c - 1)]^T$ ($[\cdot]^T$ denotes the transpose operation). The last N_g symbols of each block are copied as a

Manuscript received April 15, 2011.

Manuscript revised October 19, 2011.

[†]The authors are with the Department of Electrical and Communication Engineering, Graduate School of Engineering, Tohoku University, Sendai-shi, 980-8579 Japan.

^{††}The author is with the Department of Electric and Radio Engineering School of Electronics and Information, Kyung Hee University, Yongin-shi, Gyeonggi-do, 446-701 Republic of Korea.

a) E-mail: tenma@mobile.ecei.tohoku.ac.jp

DOI: 10.1587/transcom.E95.B.1366

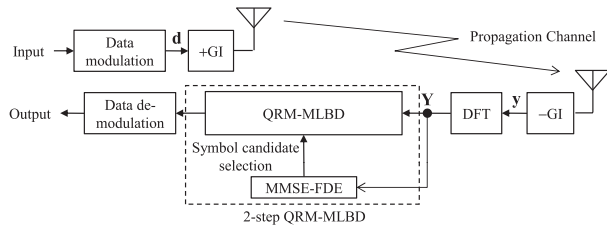


Fig. 1 SC transmission system model with 2-step QRM-MLBD.

cyclic prefix (CP) and inserted into the guard interval (GI) placed at the beginning of each block and a CP-inserted data block of $N_c + N_g$ symbols is transmitted.

We assume a symbol-spaced frequency-selective fading channel composed of L distinct propagation paths. The channel impulse response $h(\tau)$ is given by

$$h(\tau) = \sum_{l=0}^{L-1} h_l \delta(\tau - \tau_l), \quad (1)$$

where h_l and τ_l are respectively the complex-valued path gain with $E[\sum_{l=0}^{L-1} |h_l|^2] = 1$ and the time delay of the l th path. The CP-removed received signal block $\mathbf{y} = [y(0), \dots, y(N_c - 1)]^T$ can be expressed using the vector form as

$$\mathbf{y} = \sqrt{\frac{2E_s}{T_s}} \mathbf{h} \mathbf{d} + \mathbf{n}, \quad (2)$$

where E_s and T_s are respectively the symbol energy and the symbol duration, \mathbf{h} is the $N_c \times N_c$ channel impulse response matrix given as

$$\mathbf{h} = \begin{bmatrix} h_0 & & & & h_{L-1} & \dots & h_1 \\ \vdots & h_0 & & & & \ddots & \vdots \\ \vdots & \vdots & h_0 & & \mathbf{0} & & h_{L-1} \\ h_{L-1} & \vdots & \vdots & \ddots & & & \\ & h_{L-1} & \vdots & & h_0 & & \\ & & h_{L-1} & \vdots & \ddots & & \\ & & \mathbf{0} & \ddots & \vdots & \ddots & \\ & & & & h_{L-1} & \dots & h_0 \end{bmatrix}, \quad (3)$$

and $\mathbf{n} = [n(0), \dots, n(N_c - 1)]^T$ is the noise vector whose elements are the independent zero-mean Gaussian variables having the variance $2N_0/T_s$ with N_0 being the one-sided power spectrum density of additive white Gaussian noise (AWGN).

At the receiver, N_c -point DFT is applied to transform the received signal block into the frequency-domain signal vector $\mathbf{Y} = [Y(0), \dots, Y(N_c - 1)]^T$. \mathbf{Y} can be expressed as

$$\mathbf{Y} = \mathbf{F} \mathbf{y} = \sqrt{\frac{2E_s}{T_s}} \mathbf{F} \mathbf{h} \mathbf{d} + \mathbf{N}, \quad (4)$$

where $\mathbf{N} = \mathbf{F} \mathbf{n} = [N(0), \dots, N(N_c - 1)]^T$ is the frequency-domain noise vector and \mathbf{F} is the $N_c \times N_c$ DFT matrix, given

as

$$\mathbf{F} = \frac{1}{\sqrt{N_c}} \begin{bmatrix} 1 & 1 & \dots & 1 \\ 1 & e^{-j2\pi \frac{1 \times 1}{N_c}} & \dots & e^{-j2\pi \frac{1 \times (N_c-1)}{N_c}} \\ \vdots & \vdots & \ddots & \vdots \\ 1 & e^{-j2\pi \frac{(N_c-1) \times 1}{N_c}} & \dots & e^{-j2\pi \frac{(N_c-1) \times (N_c-1)}{N_c}} \end{bmatrix}. \quad (5)$$

Due to the circulant property of \mathbf{h} [17], we have

$$\mathbf{F} \mathbf{h} \mathbf{F}^H = \text{diag}[H(0), \dots, H(N_c - 1)] \equiv \mathbf{H}, \quad (6)$$

where $[\cdot]^H$ is the Hermitian transpose operation and $H(k) = \sum_{l=0}^{L-1} h_l \exp(-j2\pi k \tau_l / N_c)$. Thus, Eq. (4) can be rewritten as

$$\mathbf{Y} = \sqrt{\frac{2E_s}{T_s}} \mathbf{F} \mathbf{h} \mathbf{F}^H \mathbf{F} \mathbf{d} + \mathbf{N} = \sqrt{\frac{2E_s}{T_s}} \mathbf{H} \mathbf{d} + \mathbf{N}. \quad (7)$$

It can be understood from Eq. (7) that MLD can be done if the equivalent channel matrix (which is a concatenation of propagation channel and DFT) is known to the receiver.

2.2 Conventional QRM-MLBD

QRM-MLBD can significantly reduce the computational complexity compared to MLD. First, applying the QR decomposition to the equivalent channel matrix \mathbf{H} , we have

$$\mathbf{H} = \mathbf{Q} \mathbf{R}, \quad (8)$$

where \mathbf{Q} is an $N_c \times N_c$ unitary matrix and \mathbf{R} is an $N_c \times N_c$ upper triangular matrix. Then, multiplexing \mathbf{Y} by \mathbf{Q}^H , the transformed frequency-domain received signal \mathbf{Z} is obtained as

$$\begin{aligned} \mathbf{Z} &= [Z(0), \dots, Z(N_c - 1)]^T = \sqrt{\frac{2E_s}{T_s}} \mathbf{R} \mathbf{d} + \mathbf{Q}^H \mathbf{N} \\ &= \begin{bmatrix} R_{0,0} & R_{0,1} & \dots & R_{0,N_c-1} \\ & R_{1,1} & \dots & R_{1,N_c-1} \\ & & \ddots & \vdots \\ \mathbf{0} & & & R_{N_c-1,N_c-1} \end{bmatrix} \begin{bmatrix} d(0) \\ d(1) \\ \vdots \\ d(N_c-1) \end{bmatrix} + \mathbf{Q}^H \mathbf{N}. \end{aligned} \quad (9)$$

From Eq. (9), MLD can be expressed as

$$\begin{aligned} \mathbf{d}_{ML} &= \underset{\bar{\mathbf{d}} \in X^{N_c}}{\text{argmin}} \left(\sum_{i=1}^{N_c} \left| Z(N_c - i) - \sum_{j=1}^i \sqrt{\frac{2E_s}{T_s}} R_{N_c-i, N_c-j} \bar{d}(N_c - j) \right|^2 \right), \end{aligned} \quad (10)$$

where $\bar{\mathbf{d}} = [\bar{d}(0), \dots, \bar{d}(N_c - 1)]^T$ is the symbol candidate vector and X is the modulation level (e.g. $X = 4$ for QPSK). From Eq. (10), the ML solution can be obtained by searching for the best path having the minimum squared Euclidean distance in the tree diagram composed of N_c stages as shown in Fig. 2(a). However, MLD requires the full tree search, thus resulting in a very high computational complexity. Therefore, in QRM-MLBD, the M-algorithm [18] is used in order to reduce the complexity.

In the i th stage ($i = 0 \sim N_c - 1$) of M-algorithm, the path metric based on the squared Euclidean distance between the

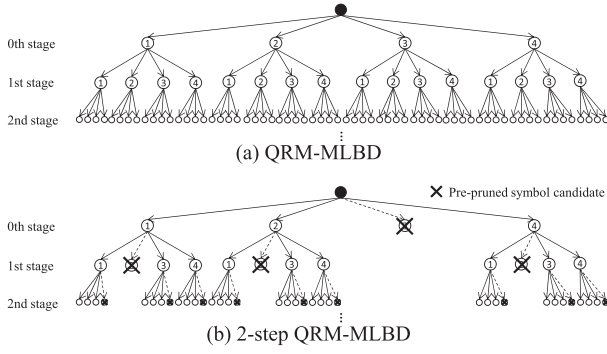


Fig. 2 Tree structure for QRM-MLBD and 2-step QRM-MLBD (QPSK case).

transformed frequency-domain received signal $Z(N_c - 1 - i)$ and the symbol candidates $\bar{d}(N_c - 1) \sim \bar{d}(N_c - 1 - i)$ is computed. The accumulated path metric, which is the sum of the path metric at the i th stage and the accumulated path metric at the $i - 1$ th stage, is obtained. Then, the best M paths are selected by comparing the accumulated path metrics associated with all surviving paths at the i th stage. This process is repeated until the last stage ($i = N_c - 1$). The most likely transmitted symbol sequence is found by tracing back along the best surviving path having the smallest accumulated path metric starting from the last stage. By using the M-algorithm, the number of path metric computations is reduced from $\sum_{n=1}^{N_c} X^n$, which is required for full ML, to $N_{cand}\{1 + M(N_c - 1)\}$, where N_{cand} denotes the average number of symbol candidates per stage to be involved in the path metric computation. In the conventional QRM-MLBD, N_{cand} is X .

2.3 2-Step QRM-MLBD

The complexity of QRM-MLBD is spent to compute the path metric, and the complexity of path metric computation for QRM-MLBD depends on the block size N_c , the number M of surviving paths at each stage and the modulation level X . In this paper, we introduce MMSE-FDE prior to QRM-MLBD to remove the symbol candidates having low reliability to reduce the computational complexity. The proposed scheme is called 2-step QRM-MLBD. In the conventional QRM-MLBD, the path metric is calculated for all X symbol candidates at each stage as shown in Fig. 2(a). In 2-step QRM-MLBD, MMSE-FDE is performed prior to QRM-MLBD to prune the paths with low reliability as shown in Fig. 2(b) and then, the M-algorithm is carried out for the pruned tree structure. In [12]–[16], methods to reduce the number of symbol candidates to be involved in the path metric computation were also proposed. However, the preliminary decision is performed successively in the M-algorithm and therefore the decision reliability in early stages is likely to be low because the elements of \mathbf{R} closer to the right positions tend to drop with larger probability in single carrier transmission [19]. By contrast, in 2-step QRM-MLBD, unreliable symbol candidates are discarded from the tree

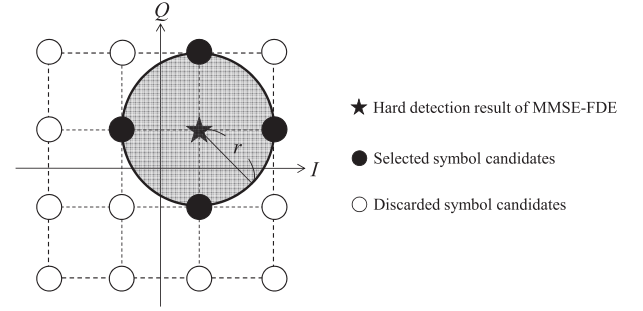


Fig. 3 Symbol candidate selection (16QAM case).

shown in Fig. 2, based on the preliminary decision using MMSE-FDE, prior to conducting the M-algorithm. Consequently, by using 2-step QRM-MLBD, more accurate decision can be done in early stages compared to methods in [12]–[16].

(a) First step

MMSE-FDE is carried out as [3]

$$\tilde{\mathbf{D}} = \mathbf{W}\mathbf{Y}, \quad (11)$$

where \mathbf{Y} is the frequency-domain received signal given by

$$\mathbf{Y} = \sqrt{\frac{2E_s}{T_s}} \mathbf{H}\mathbf{D} + \mathbf{N} \quad (12)$$

with $\mathbf{D} = \mathbf{F}\mathbf{d}$ being the frequency-domain transmitted signal vector and

$$\mathbf{W} = \text{diag} \left[\frac{H^*(0)}{|H(0)|^2 + (E_s/N_0)^{-1}}, \dots, \frac{H^*(N_c-1)}{|H(N_c-1)|^2 + (E_s/N_0)^{-1}} \right] \quad (13)$$

is the MMSE weight [2, 3]. $[\cdot]^*$ denotes the complex conjugate operation. Next, the time-domain received symbol vector $\tilde{\mathbf{d}}$ is obtained by applying N_c point inverse DFT (IDFT) as

$$\tilde{\mathbf{d}} = \mathbf{F}^H \tilde{\mathbf{D}}. \quad (14)$$

Then, hard decision is done on $\tilde{\mathbf{d}}$.

The symbol candidates within distance r from the MMSE-FDE hard detection result are selected and the others are discarded. In this way, the symbol candidates having low reliability are removed from the tree. Figure 3 shows how to select the symbol candidates for the 16QAM case. However, the use of too small r leads to BER performance degradation. Hence, there is a trade-off relationship between the complexity reduction and BER performance.

(b) Second step

The M-algorithm is carried out. As the paths with low reliability have already been pruned in the first step, the complexity of path metric computation is reduced compared to the conventional QRM-MLBD. Reducing the number of symbol candidates by drawing a circle is similar to sphere decoding (SD) [20]. The difference between 2-step QRM-MLBD and SD is discussed in the Appendix.

3. Computer Simulation

The computer simulation condition is shown in Table 1. Block size of $N_c = 64$, and GI size of $N_g = 16$ are assumed. The channel is assumed to be a frequency-selective block Rayleigh fading channel having symbol-spaced $L = 16$ -path uniform power delay profile. Ideal estimation of the channel and noise power is assumed. First, we find the optimum r . Then, we show the BER performance achievable with 2-step QRM-MLBD and compare it with the conventional QRM-MLBD.

3.1 Optimization of r

In order to find the optimum r , we measured the *a posteriori* probability distribution of transmitted symbols when MMSE-FDE is used. Since the signal constellation is circularly symmetric, it is sufficient to measure the *a posteriori* probability distribution of transmitted symbols for the case of the hard detection result of MMSE-FDE falling in the first quadrant.

The *a posteriori* probability distribution obtained by the computer simulation is plotted in Figs. 4, 5, and 6 at the average received bit energy-to-noise power spectrum density ratio $E_b/N_0 (= (E_s/N_0)(1 + N_g/N_c)/\log_2 X)$ value necessary to achieve BER $\approx 10^{-3}$ by QRM-MLBD for QPSK, 16QAM and 64QAM, respectively. The average received E_b/N_0 is set to 10, 14, and 18 dB for QPSK, 16QAM, and 64QAM, respectively. In the case of QPSK, it can be seen from Fig. 4 that the *a posteriori* probability of the most distant symbol is quite low and therefore, $r = \sqrt{2}$ can be used as shown in Fig. 7(a). In the 16QAM case, it is seen from Fig. 5 that the *a posteriori* probability of the symbols located

outside a circle having a radius of $2/\sqrt{5}$ centering the hard detection result of MMSE-FDE is negligibly small. Therefore, $r = 2/\sqrt{5}$ can be used. In this paper, for comparison, the BER performance of 2-step QRM-MLBD using $r = 2/\sqrt{10}$ and $4/\sqrt{10}$ are compared as shown in Fig. 7(b). Also, in the 64QAM case, it can be seen from Fig. 6 that the *a posteriori* probability located outside a circle having the radius $2/\sqrt{21}$ centering the hard detection result of MMSE-FDE is negligible. Therefore, $r = 2/\sqrt{21}$ can be used. In the 64QAM case, we evaluate the BER performance of 2-step QRM-MLBD with $r = 2/\sqrt{42}$ and $4/\sqrt{42}$ as shown in Fig. 7(c).

3.2 BER Performance

The average BER performance of 2-step QRM-MLBD using $r = 2/\sqrt{10}$, $2/\sqrt{5}$, and $4/\sqrt{10}$ for 16QAM ($X = 16$) and using $r = 2/\sqrt{42}$, $2/\sqrt{21}$, and $4/\sqrt{42}$ for 64QAM ($X = 64$) are plotted in Figs. 8 and 9, respectively, as a function of the

Table 1 Computer simulation condition.

Transmitter	Modulation	QPSK, 16QAM, 64QAM
	Block size	$N_c = 64$
	GI	$N_g = 16$
Channel	Fading type	Frequency-selective block Rayleigh
	Power delay profile	$L = 16$ -path uniform
	Time delay	$\tau_l = l(l = 0 \sim L - 1)$
Receiver	Channel estimation	Ideal
	Noise power estimation	

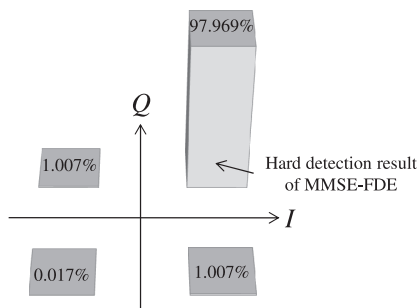


Fig. 4 *A posteriori* probability distribution for QPSK. $E_b/N_0=10$ dB.

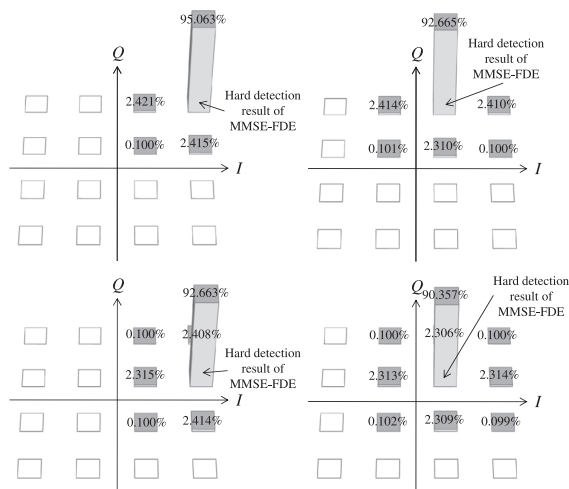


Fig. 5 *A posteriori* probability distribution for 16QAM. $E_b/N_0=14$ dB.

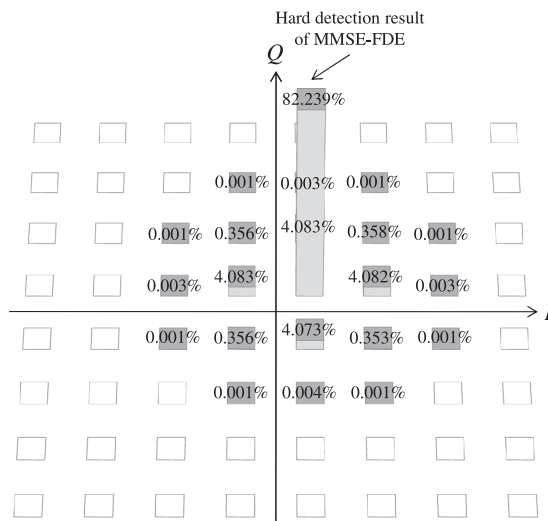


Fig. 6 *A posteriori* probability distribution for 64QAM. $E_b/N_0=18$ dB.

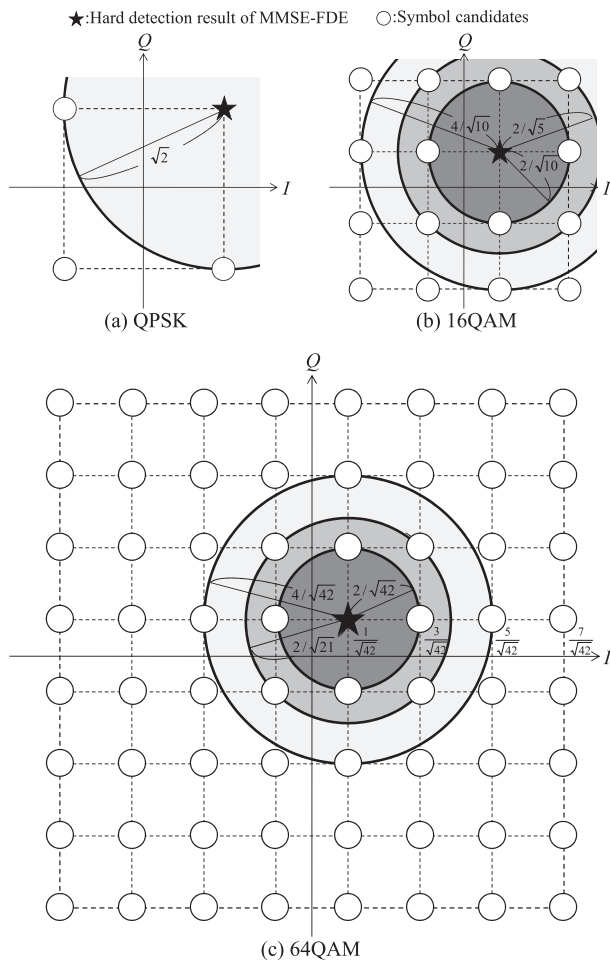


Fig. 7 Symbol candidate selection.

average received E_b/N_0 . In the 16QAM case, when $M = 16$, although the difference is very small, the use of $r = 2/\sqrt{5}$ is superior to the others. The BER performance of QRM-MLBD degrades when using a smaller number M of surviving paths in the M-algorithm (e.g., $M = 16$ for 16QAM) since the probability of discarding the correct path at early stages increases. In 2-step QRM-MLBD, unreliable symbol candidates are discarded based on MMSE-FDE decision prior to conducting the M-algorithm. Hence, the probability of discarding the correct path in early stages can be reduced and the BER performance can be improved compared to QRM-MLBD when a small M is used. Using $r = 2/\sqrt{5}$, a larger number of symbol candidates can be kept than in the case of $r = 4/\sqrt{10}$ and therefore, the probability of discarding the correct path in early stages increases. This is the reason why the BER performance of 2-step QRM-MLBD with $r = 2/\sqrt{5}$ is slightly superior to that with $r = 4/\sqrt{10}$. However, the performance difference diminishes when $M = 256$.

If $r = 2/\sqrt{10}$ is used, the BER performance degrades even in the high E_b/N_0 region for both $M = 16$ and $M = 256$. In the high E_b/N_0 region, the average BER performance of MMSE-FDE considerably degrades compared to that of QRM-MLBD. Therefore, if a small radius r is used,

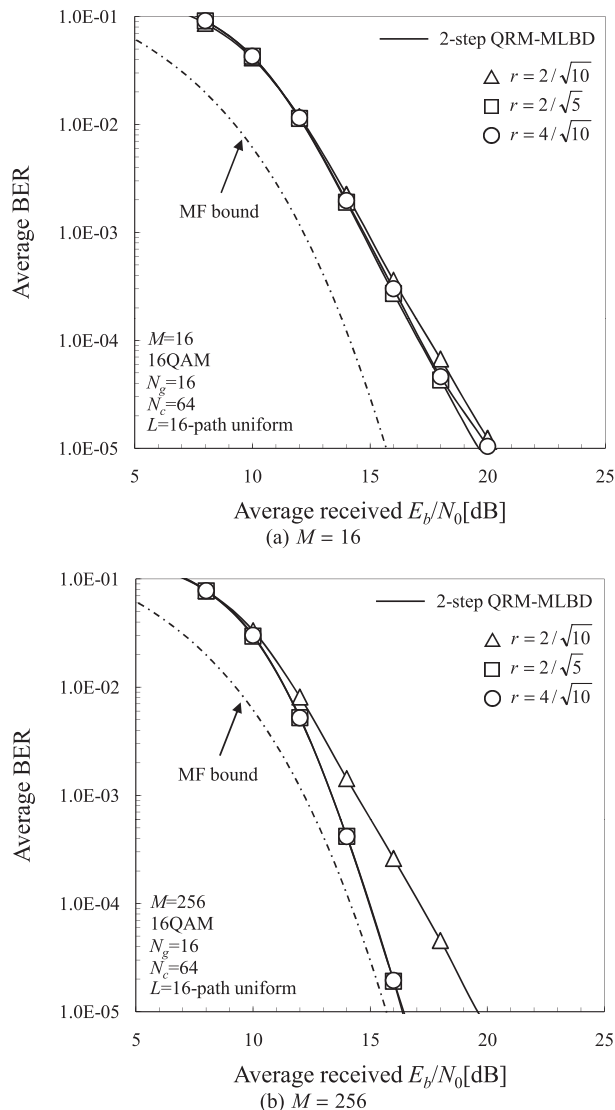


Fig. 8 BER performance of 2-step QRM-MLBD for 16QAM.

the correct symbol candidates may be discarded prior to conducting the M-algorithm and hence, the average BER performance of 2-step QRM-MLBD degrades even if a large M is used. In the 64QAM case, if $r = 2/\sqrt{42}$ is used, the BER performance becomes inferior to others for same reason noted above when $M = 16$ and $M = 256$. This is particularly true for the former one, namely $r = 2/\sqrt{21}$ case is superior to others.

Figure 10 shows the BER as a function of r for $E_b/N_0 = 8, 12$ and 14 dB (respectively $12, 16$ and 18 dB) which are necessary to achieve $BER \approx 10^{-1}, 10^{-2}$ and 10^{-3} for 16QAM (respectively 64QAM). It can be seen from Fig. 10 that when $E_b/N_0 = 8$ dB for 16QAM (respectively 12 dB for 64QAM), the BER performance is almost the same for the three r cases. However, when $E_b/N_0 = 12$ and 14 dB for 16QAM (respectively 16 and 18 dB for 64QAM), the use of the smallest r gives inferior performance. As a consequence, the smallest radius can be used in the low E_b/N_0 re-

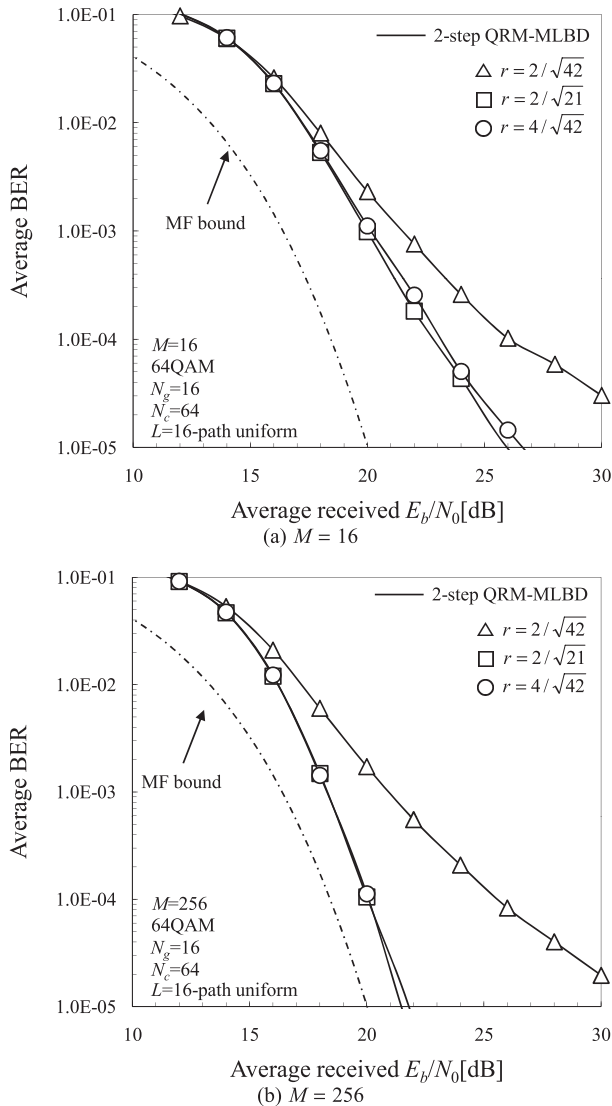


Fig. 9 BER performance of 2-step QRM-MLBD for 64QAM.

gion while larger radius should be used in the higher E_b/N_0 region. Therefore, in this paper we use $r = 2/\sqrt{5}$ for 16QAM and $r = 2/\sqrt{21}$ for 64QAM in all E_b/N_0 regions.

Figure 11 shows the BER performance comparison between 2-step QRM-MLBD and the conventional QRM-MLBD. Three cases of M are plotted, i.e., $M = 4, 16$, and 64 for QPSK and $M = 16, 64$, and 256 for 16QAM and 64QAM. Also plotted for comparison are the MF bound [21] and the BER performance of MMSE-FDE. r is set to $\sqrt{2}$ for QPSK, $2/\sqrt{5}$ for 16QAM and $2/\sqrt{21}$ for 64QAM.

First, the case of QPSK is discussed. It can be seen from Fig. 11(a) that 2-step QRM-MLBD using $M = 4$ provides better BER performance than conventional QRM-MLBD. This is because the symbol candidates having low reliability have been already discarded in the first step and therefore, the probability of discarding the correct path in the M-algorithm gets lower than the conventional QRM-MLBD. However, when M is increased to 64, 2-step QRM-

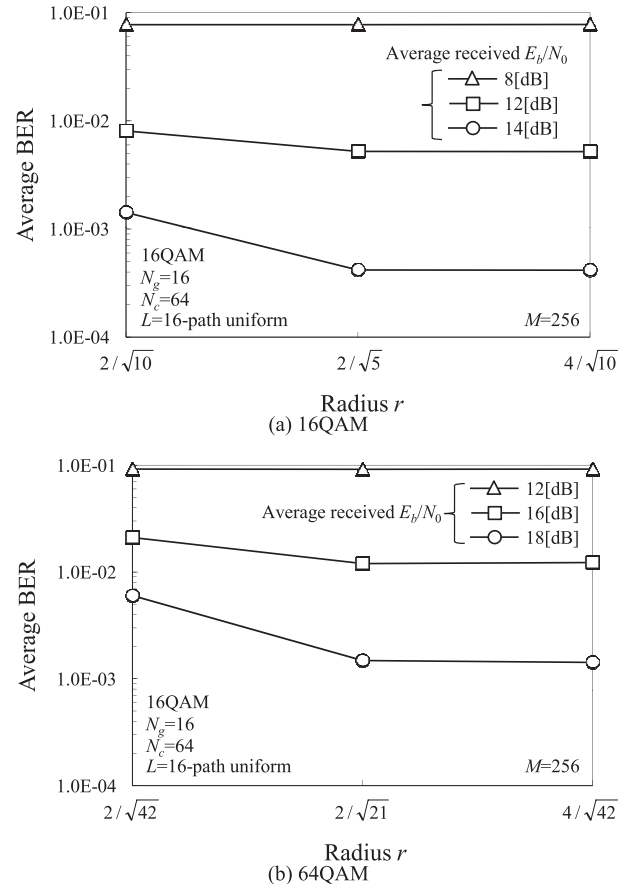


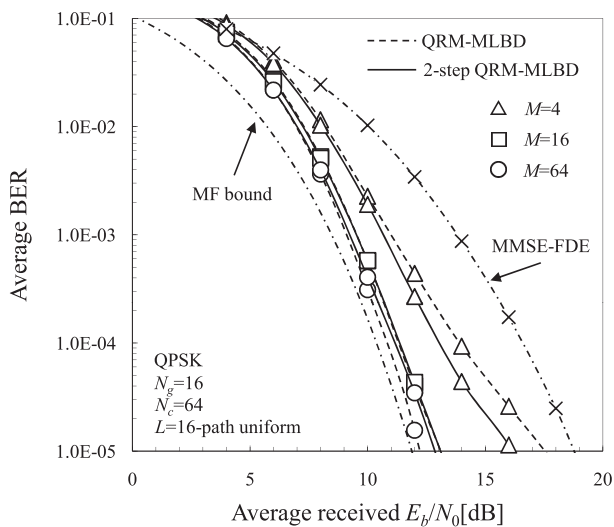
Fig. 10 Impact of r on average BER.

MLBD provides slightly degraded performance. This slight performance degradation is a cause of removing the correct symbol in the first step. However, this degradation is unnoticeable when M is small.

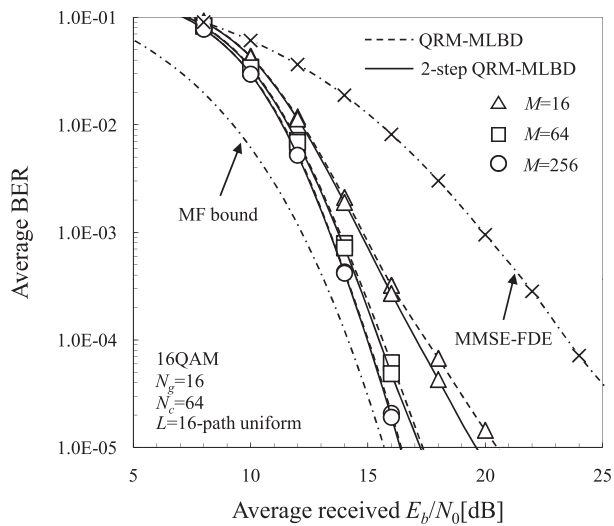
Next, we discuss the cases of 16QAM and 64QAM. It can be seen from Figs. 11(b) and 11(c) that 2-step QRM-MLBD can achieve slightly better BER performance than the conventional QRM-MLBD for the same reason as in the QPSK case.

3.3 Computational Complexity

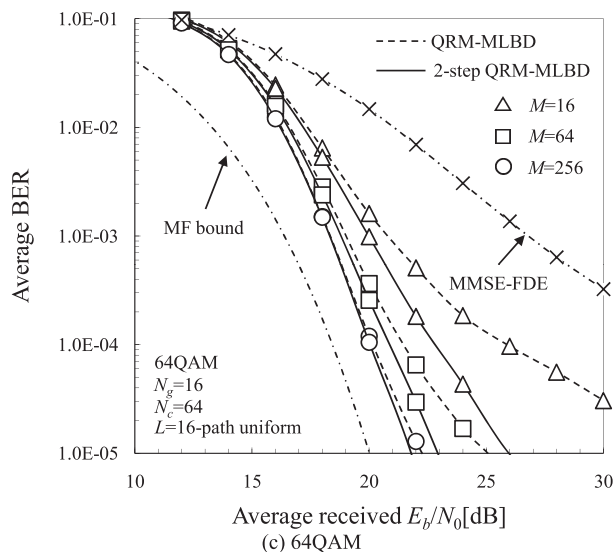
The computational complexity of the 2-step QRM-MLBD, in terms of the number of complex multiply operations, is compared with those of QRM-MLBD and MMSE-FDE. Table 2 shows the computational complexity. The complexity of path metric computation in conventional QRM-MLBD is $N_{cand}(2 + (M/2)(N_c + 4)(N_c - 1))$, where N_{cand} is always set to 4 for QPSK, 16 for 16QAM, and 64 for 64QAM. In this paper, the radius is set $r = \sqrt{2}$, $2/\sqrt{5}$ and $2/\sqrt{21}$ for QPSK, 16QAM, and 64QAM, respectively so that the BER performance closest to the MF bound can be achieved. Therefore, when all possible symbols are transmitted with equal probability, the average N_{cand} can be reduced to 3, 6.3, and 7.6 for QPSK, 16QAM, and 64QAM, respectively. As a result, 2-



(a) QPSK



(b) 16QAM



(c) 64QAM

Fig. 11 BER performance comparison between 2-step QRM-MLBD and conventional QRM-MLBD.

Table 2 Number of complex multiply operations.

	MMSE-FDE	QRM-MLBD	2-step QRM-MLBD
Fast Fourier transform (FFT)	$N_c \log_2 N_c$		
MMSE-weight computation & FDE	$N_c + N_c$		$N_c + N_c$
Inverse FFT (IFFT)	$N_c \log_2 N_c$		$N_c \log_2 N_c$
HF computation & QR decomposition	$N_c^2 + N_c^3$		
Q^H multiplication	N_c^2		
Path metric computation		$N_{cand} = X$	$N_{cand} = 3, 6.3, 7.6$ for QPSK, 16QAM, and 64QAM, respectively
		$N_{cand} \{2 + (M/2)(N_c + 4)(N_c - 1)\}$	

step QRM-MLBD can reduce the total amount of computational complexity compared to conventional QRM-MLBD. If we want to achieve a near MF bound performance, we need to use $M = 64$ for QPSK and $M = 256$ for both 16QAM and 64QAM; the total computational complexity of 2-step QRM-MLBD can be reduced to 83%, 41% and 13% of conventional QRM-MLBD for QPSK, 16QAM and 64QAM, respectively.

4. Conclusion

In this paper, we proposed the computationally efficient 2-step QRM-MLBD; it uses MMSE-FDE before QRM-MLBD in order to reduce the number of symbol candidates. In 2-step QRM-MLBD, the symbol candidates outside a circle of radius r from the hard decision of MMSE-FDE are discarded. We found the optimum value of r using the *a posteriori* probability of transmitted symbols when MMSE-FDE is used. We showed that 2-step QRM-MLBD can reduce the computational complexity to about 83%, 41%, and 13% of the conventional QRM-MLBD for QPSK, 16QAM, and 64QAM, respectively.

The computational complexity of 2-step QRM-MLBD is still high compared to MMSE-FDE. For example, 2-step QRM-MLBD requires about 4,000 times higher computational complexity than MMSE-FDE to achieve a near MF bound performance for 16QAM. Further complexity reduction is an important future study topic. In addition, we did not consider any error correcting coding scheme in this paper. A study of error correcting coded case is left as a future study topic.

References

- [1] J.G. Proakis and M. Salehi, Digital communications, 5th ed., McGraw-Hill, 2008.
- [2] D. Falconer, S.L. Ariyavisitakul, A. Benyamin-Seeyar, and B. Edison, "Frequency domain equalization for single-carrier broadband wireless systems," IEEE Commun. Mag., vol.40, no.4, pp.58-66, April 2002.
- [3] F. Adachi, T. Sao, and T. Itagaki, "Performance of multicode DS-CDMA using frequency domain equalization in a frequency selective fading channel," Electron. Lett., vol.39, no.2, pp.239-241, Jan.

- 2003.
- [4] K. Takeda, K. Ishihara, and F. Adachi, "Frequency-domain ICI cancellation with MMSE equalization for DS-CDMA downlink," *IEICE Trans. Commun.*, vol.E89-B, no.12, pp.3335–3343, Dec. 2006.
 - [5] A. van Zelst, R. van Nee, and G.A. Awater, "Space division multiplexing (SDM) for OFDM systems," *Proc. IEEE 51st Vehicular Technology Conference (VTC2000-Spring)*, pp.1070–1074, May 2000.
 - [6] L.J. Kim and J. Yue, "Joint channel estimation and data detection algorithms for MIMO-OFDM systems," *Proc. 36th Asilomar Conference on Signals, System and Computers*, pp.1857–1861, Nov. 2002.
 - [7] T. Yamamoto, K. Takeda, and F. Adachi, "Single-carrier transmission using QRM-MLD with antenna diversity," *Proc. 12th International Symposium on Wireless Personal Multimedia Communications (WPMC 2009)*, Sept. 2009.
 - [8] K. Nagatomi, K. Higuchi, and H. Kawai, "Complexity reduced MLD based on QR decomposition in OFDM-MIMO multiplexing with frequency domain spreading and code multiplexing," *Proc. IEEE Wireless Communication & Networking Conference (WCNC 2009)*, pp.1–6, April 2009.
 - [9] T. Yamamoto, K. Takeda, and F. Adachi, "Training sequence aided single-carrier block signal detection using QRM-MLD," *Proc. IEEE Wireless Communication & Networking Conference (WCNC 2010)*, pp.1–6, April 2010.
 - [10] T. Yamamoto, K. Takeda, and F. Adachi, "MMSE based QRM-MLD frequency-domain block signal detection for single-carrier transmission," *Proc. 7th IEEE VTS Asia Pacific Wireless Communication Symposium (APWCS 2010)*, May 2010.
 - [11] H. Kawai, K. Higuchi, N. Maeda, and M. Sawahashi, "Adaptive control of surviving symbol replica candidates in QRM-MLD for OFDM MIMO multiplexing" *IEEE J. Sel. Areas Commun.*, vol.24, no.6, pp.1130–1140, June 2006.
 - [12] X. Duan, G. Ren, L. Yang, and G. Yu, "Low complexity QRM-MLD algorithm for MIMO systems with 256 QAM modulations," *International Conference on Communication Technology Proceedings*, pp.1052–1055, 2010.
 - [13] B.-S. Kim and K. Choi, "A very low complexity QRD-m algorithm based on limited tree search for MIMO systems," *IEEE Vehicular Technology Conference*, pp.1246–1250, 2008.
 - [14] X. Xin, X. Li, Y. Hei, W. Yin, and G. Yu, "A modified QRD-M algorithm based on layer branch pruning for MIMO systems," *International Conference on Advanced Information Networking and Applications*, pp.461–464, 2010.
 - [15] T.-H. Im, J. Kim, and Y.-S. Cho, "A computationally efficient modification of QRM-MLD signal detection method," *IEICE Trans. Commun.*, vol.E92-B, no.4, pp.1365–1368, April 2009.
 - [16] H. Hur, H. Woo, W.-Y. Yang, S. Bahng, Y.-O. Park, and J. Kim, "A computationally efficient search space for QRM-MLD signal detection," *IEICE Trans. Commun.*, vol.E92-B, no.3, pp.1045–1048, March 2009.
 - [17] G.H. Golub and C.F. van Loan, *Matrix Computations*, 3rd ed., Johns Hopkins Univ. Press, Baltimore, MD, 1996.
 - [18] J.B. Anderson and S. Mohan, "Sequential coding algorithms: A survey and cost analysis," *IEEE Trans. Commun.*, vol.32, no.2, pp.169–176, Feb. 1984.
 - [19] K. Takeda, H. Tomeba, and F. Adachi, "Joint Tomlinson-Harashima precoding and frequency-domain equalization for broadband single-carrier transmission," *IEICE Trans. Commun.*, vol.E91-B, no.1, pp.258–266, Jan. 2008.
 - [20] E. Viterbo and J. Boutros, "A universal lattice code decoder for fading channel," *IEEE Trans. Inf. Theory*, vol.45, no.5, pp.1639–1642, July 1999.
 - [21] F. Adachi and K. Takeda, "Bit error rate analysis of DS-CDMA with joint frequency-domain equalization and antenna diversity combining," *IEICE Trans. Commun.*, vol.E87-B, no.10, pp.2991–3002, Oct. 2004.
 - [22] K.-C. Lai and L.-W. Lin, "Low-complexity adaptive tree search

algorithm for MIMO detection," *IEEE Trans. Wireless Commun.*, vol.8, no.7, pp.3716–3726, July 2009.

Appendix: Algorithm Comparison with Sphere Decoding

SD can be represented as

$$\left\| \mathbf{Z} - \sqrt{\frac{2E_s}{T_s}} \mathbf{R} \mathbf{d} \right\|^2 \leq C^2 \quad (\text{A} \cdot 1)$$

where C denotes the radius of the $2N_c$ -dimensional hypersphere. The difference between 2-step QRM-MLBD and SD [20] is two-fold.

First, the sphere in SD is different from that of 2-step QRM-MLBD. SD draws the $2N_c$ -dimensional hypersphere which is centered in the transformed received signal sequence \mathbf{Z} and searches the symbol candidate sequences inside the hypersphere. If there are no symbol candidate sequences inside the hypersphere, the radius of hypersphere is expanded to start the tree search again. On the other hand, 2-step QRM-MLBD limits the search symbol candidates at each tree stage by drawing the 2-dimensional sphere (i.e. circle) in the I - Q plane.

Second, the tree search algorithm is different. SD employs the depth-first search while 2-step QRM-MLBD (and also conventional QRM-MLBD) employs the breadth-first search [22].

SD can achieve the same BER performance as MLD. This is because the hypersphere certainly includes the symbol candidate sequences with minimum squared Euclidean distance from the received signal. 2-step QRM-MLBD, on the other hand, has a possibility to discard the correct path. 2-step QRM-MLBD uses the M-algorithm to reduce the computational complexity, but does not guarantee to always achieve the MLD performance.



Katsuhiko Temma received his B.S. degree in Electrical, Information and Physics Engineering in 2010 from Tohoku University, Sendai, Japan. Currently he is a graduate student at the Department of Electrical and Communications Engineering, Tohoku University. His research interests include frequency-domain equalization and signal detection techniques for mobile communication systems.



Tetsuya Yamamoto received his B.S. degree in Electrical, Information and Physics Engineering in 2008 and M.S. degree in communications engineering, in 2010, respectively, from Tohoku University, Sendai Japan. Currently he is a Japan Society for the Promotion of Science (JSPS) research fellow, studying toward his Ph.D. degree at the Department of Electrical and Communications Engineering, Graduate School of Engineering, Tohoku University. His research interests include frequency-domain equalization

and signal detection techniques for mobile communication systems. He was a recipient of the 2008 IEICE RCS (Radio Communication Systems) Active Research Award.



KyeSan Lee received a B.E. degree in electrical engineering from Kyung Hee University in Korea and M.S. and Ph.D. degrees from the department of electrical engineering, Keio University, Yokohama, Japan, in 1996, 1999, and 2002, respectively. He joined KDDI R&D Laboratories Inc. in 2002 and has received an IEEE VTS Japan young researchers encouragement award. Since 2003, he has been with the College of Electronic and Information, Kyung Hee University, where he is a Professor. His research

interests include wireless communication network, CDMA, OFDM, MC-CDMA, MIMO, and Cognitive radio and Visible Light Communication systems.



FumiYuki Adachi received the B.S. and Dr. Eng. degrees in electrical engineering from Tohoku University, Sendai, Japan, in 1973 and 1984, respectively. In April 1973, he joined the Electrical Communications Laboratories of Nippon Telegraph & Telephone Corporation (now NTT) and conducted various types of research related to digital cellular mobile communications. From July 1992 to December 1999, he was with NTT Mobile Communications Network, Inc. (now NTT DoCoMo, Inc.), where he

led a research group on wideband/broadband CDMA wireless access for IMT-2000 and beyond. Since January 2000, he has been with Tohoku University, Sendai, Japan, where he is a Professor of Electrical and Communication Engineering at the Graduate School of Engineering. His research interests are in CDMA wireless access techniques, equalization, transmit/receive antenna diversity, MIMO, adaptive transmission, and channel coding, with particular application to broadband wireless communications systems. From October 1984 to September 1985, he was a United Kingdom SERC Visiting Research Fellow in the Department of Electrical Engineering and Electronics at Liverpool University. He is an IEICE Fellow and was a co-recipient of the IEICE Transactions best paper of the year award 1996 and again 1998 and also a recipient of Achievement award 2003. He is an IEEE Fellow and was a co-recipient of the IEEE Vehicular Technology Transactions best paper of the year award 1980 and again 1990 and also a recipient of Avant Garde award 2000. He was a recipient of Thomson Scientific Research Front Award 2004 and Ericsson Telecommunications Award 2008.